Three-dimensional chiral photonic superlattices

M. Thiel,[1,*] H. Fischer,[2] G. von Freymann,[1,3] and M. Wegener[1,3]

[1]*Institut für Angewandte Physik and DFG-Center for Functional Nanostructures (CFN), Karlsruhe Institute of Technology (KIT), D-76128 Karlsruhe, Germany*
[2]*Nanoscribe GmbH, D-76344 Eggenstein-Leopoldshafen, Germany*
[3]*Institut für Nanotechnologie, Karlsruhe Institute of Technology (KIT), Hermann-von-Helmholtz-Platz 1, D-76344 Eggenstein-Leopoldshafen, Germany*
**Corresponding author: michael.thiel@physik.uni-karlsruhe.de*

Received October 29, 2009; revised November 25, 2009; accepted December 7, 2009; posted December 14, 2009 (Doc. ID 119295); published January 13, 2010

We investigate three-dimensional photonic superlattices composed of polymeric helices in various spatial checkerboard-like arrangements. Depending on the relative phase shift and handedness of the chiral building blocks, different circular-dichroism resonances appear or are suppressed. Samples corresponding to four different configurations are fabricated by direct laser writing. The measured optical transmittance spectra are in good agreement with numerical calculations. © 2010 Optical Society of America

OCIS codes: 160.1585, 160.5298, 160.3918, 220.4241, 260.5430.

Recently, an increasing number of researchers have been designing, fabricating, and studying artificial chiral dielectric [1–9] or metallic [10–15] materials. These man-made media allow for optical activity or circular dichroism as obtained for chiral molecules, however, with coefficients that are orders of magnitude larger. Furthermore, qualitatively new effects can occur, for example, negative phase velocities [10,11] or negative reflection [12]. Potential applications have been discussed and range from circular polarizers [6,7,15] to optical diodes and/or poor-man's optical isolators [16].

The resonances in chiral dielectric structures have been interpreted following the lines of cholesteric liquid crystals: A resonance occurs if the spiral (strictly helix) pitch equals the effective material wavelength [6–8]. In this simple intuitive picture, which is essentially based on individual spirals, the interaction between adjacent spirals is completely neglected. In this Letter, we aim at investigating these lateral interactions. To allow for an unambiguous interpretation, we change only the relative phase of neighboring spirals or their handedness.

The geometry of our model system is illustrated in Fig. 1. All extended unit cells are composed of four spirals with the same structural parameters but with a varying phase or handedness in a checkerboard-like manner. While four spirals with the same handedness are laterally arranged in case I, they are phase shifted by 90° in case II, and by 180° in case III. These cases are enantiopure configurations. In case IV, the handedness alternates, resulting in a racemic mixture of chiral helices. The distance between adjacent spirals a and the spiral diameter $L=0.9a$ are fixed. $2a$ is the in-plane lattice constant. These extended unit cells are stacked to a three-dimensional photonic crystal with $N=7$ axial lattice constants. As an example, the resulting structure of case II is shown in Fig. 1(b).

To fabricate such complex photonic superlattices, we employ a commercially available direct-laser-writing system (Nanoscribe Photonic Professional) to expose the negative-tone photoresist SU-8 (details

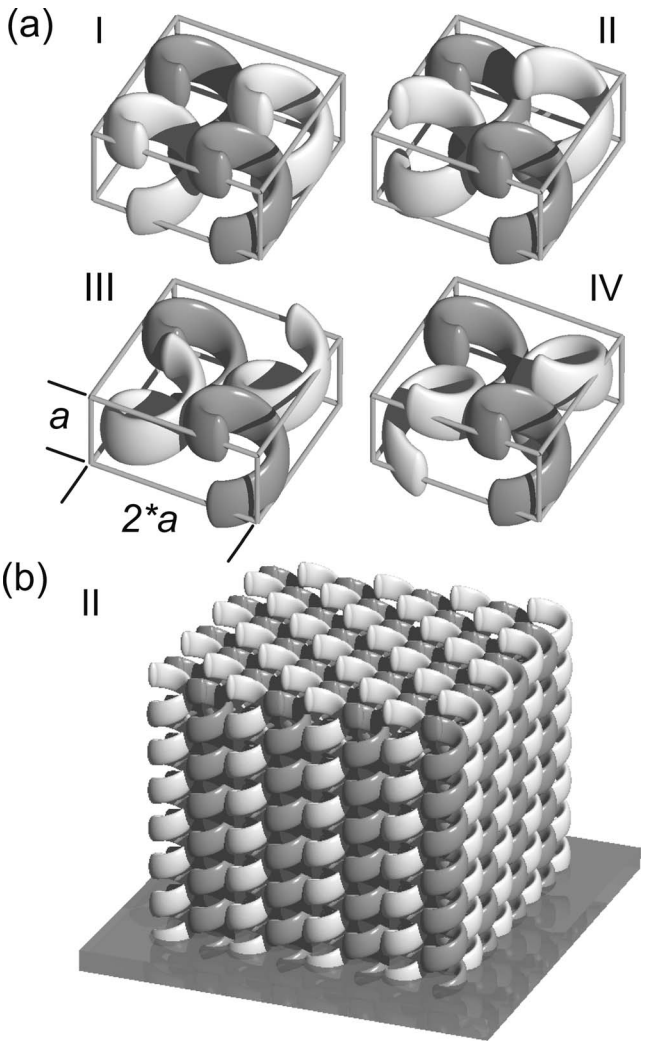

Fig. 1. (a) Four configurations of chiral photonic crystals: Spirals with the same handedness are in phase (I), 90° out of phase (II), and 180° out of phase (III). Configuration IV is a racemic mixture of helices. Each spiral is situated in a cubic unit cell with lattice constant a. (b) Oblique view on a chiral photonic superlattice of configuration II with $N=7$ axial periods.

0146-9592/10/020166-3/$15.00

can be found in [9]). The parameters are $a=3.25\ \mu m$, $L=2.925\ \mu m$, and a volume filling fraction of 36.5%. All fabricated structures have a footprint of 65 $\mu m \times 65\ \mu m$ and have been fabricated under identical conditions on the same glass slide. Top-view electron micrographs of each superlattice are depicted in Fig. 2(a). The four different configurations correspond to those shown in Fig. 1. To demonstrate the high quality and homogeneity, an oblique view of a circular-spiral photonic crystal of case II is shown in Fig. 2(b).

The optical properties of the chiral photonic crystals of case I have previously been discussed in detail in [6,7]. The resulting polarization stop bands have been interpreted intuitively following the above simple picture. In this picture, the optical properties of cases I–III should be identical. In contrast, the chiral effects are expected to disappear in case IV [8].

The measured optical transmittance spectra of the sample shown in Fig. 2 are shown in Fig. 3 (left column). All spectra are taken by using a Fourier-transform microscope-spectrometer (Bruker Tensor 27 with Hyperion 1000 microscope). We use circular polarization of the incident light achieved by a high-extinction wire-grid polarizer (Bruker) and a super-achromatic quarter-wave-plate (Bernhard Halle Nachfl.) granting access to the spectral regime of 2.5–7.0 μm wavelength [9]. The full opening angle of the incident light impinging under nominally normal incidence is reduced to about 5° by means of a diaphragm. All spectra are referenced to the bare glass substrate.

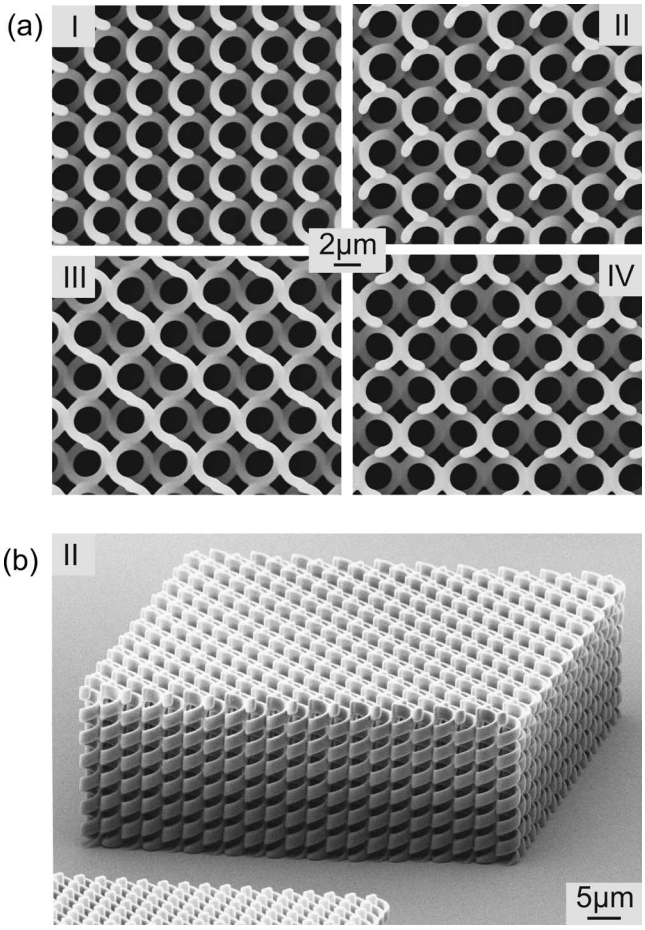

Fig. 2. (a) Top-view electron micrographs of fabricated circular-spiral photonic crystals in the same order as shown in Fig. 1. (b) Oblique-view electron micrograph of a polymer structure of configuration II fabricated by direct laser writing. The cubic lattice constant of all structures is $a=3.25\ \mu m$, their footprint is 65 $\mu m \times 65\ \mu m$, and they contain seven lattice constants normal to the glass substrate plane. Each spiral diameter is $L=0.9a$.

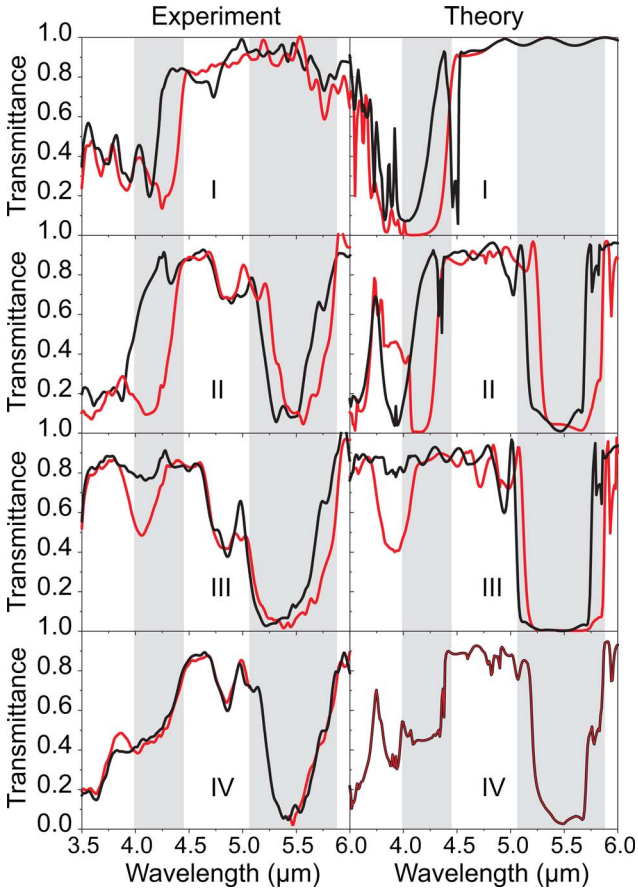

Fig. 3. (Color online) Transmittance spectra of the samples shown in Fig. 2 taken/calculated under normal incidence for circular polarization of the incident light. Left-handed (black curves) and right-handed [gray (red online) curves] circular polarizations of the incident light are shown for all four different configurations (I–IV). The gray areas highlight stop bands for circular polarization or polarization-independent stop band.

Case I reveals the previously discussed polarization stop band for circular polarization centered on 4.3 μm. The details are different because the adjacent spirals slightly overlap in this Letter, whereas they have been well separated previously [7]. We have chosen overlapping spirals in this Letter in order to ensure mechanical stability without the need for additional stabilization (grids and wall in [7]). In contrast to case I, the optical properties of cases II and III considerably differ from the expectations from the simple picture. In particular, in both cases, a second additional set of longer-wavelength resonances appears. Again, the stop band depends on the circular polarization leading to circular dichroism. Furthermore, in case III, the original polarization stop band has been strongly suppressed, whereas it is still visible in case II. Alas, the above simple picture

taken from cholesteric liquid crystals is not sufficient to describe the observed behavior, especially the additional longer-wavelength resonance. Interestingly, this additional stop band occurs at a wavelength that is about a factor of $\sqrt{2}$ larger than that of the original polarization stop band. This factor correlates with the in-plane distance between adjacent equivalent spirals which is a in case I and $\sqrt{2}a$ in cases II and III. Finally, the racemic mixture (case IV) hardly shows any chiral response. Nevertheless, the longer-wavelength stop band also seen in cases II and III is still present.

To further investigate the optical properties and to rule out experimental artifacts, we perform numerical calculations based on the well-established scattering-matrix approach [17,18]. This approach is capable of calculating the transmittance spectra of finite-size structures. We choose normally incident circular polarization of light [black for left-circular and gray (red online) for right-circular], a polymer refractive index of $n=1.57$, a refractive index of the semi-infinite glass substrate of $n=1.518$, and the geometrical structure parameters of the fabricated structures shown in Fig. 2. In particular, we also account for the elongated point-spread function of the direct laser writing (aspect ratio of 2.7). The lateral and axial discretization of each unit cell is set to $a/128=25.4$ nm. We use $g=7$ orders corresponding to $(2g+1)^2=225$ reciprocal lattice vectors. The normal-incidence intensity transmittance refers to the (0,0) diffraction order. The transmittance differences between $g=7$ and 8 are within the linewidth of the shown curves (smaller than 0.015), indicating that the numerical results converge. The results are shown in the right column of Fig. 3, allowing for a direct comparison with experiment in the other column.

The overall qualitative agreement between theory and experiment is good. Specifically, the spectral positions of the stop bands and the depth of the transmittance minima are reproduced rather well. Remaining quantitative deviations likely arise from (i) slight imperfections of the fabricated structures and/or (ii) from the finite opening angle of the measurement apparatus. Regarding aspect (i), we have already noted above that all four samples have been fabricated on one glass substrate under identical conditions allowing for a fair comparison of the four different fabricated samples. Typically, further slight improvements can be achieved when optimizing the samples individually. The importance of aspect (ii) has been emphasized previously [7] by comparison of calculated spectra for strictly normal incidence and spectra averaged over a certain opening angle (5°, see above). The angle averaging tends to smear out sharp spectral features. In this Letter, we show normal-incidence data to reveal the intrinsic optical response.

In conclusion, we have presented three-dimensional chiral photonic superlattices composed of different checkerboard-like arrangements of polymer spirals. We have found that the chiral optical properties strongly depend on the in-plane arrangement of the spirals rather than solely on the spiral parameters. This opens what we believe to be new design options for tailoring the optical properties of these artificial chiral structures. Furthermore, this observation highlights the differences in the physics of cholesteric liquid crystals and helical photonic crystals.

We thank M. S. Rill for valuable comments on the manuscript. We acknowledge support by the Deutsche Forschungsgemeinschaft (DFG) and the State of Baden-Württemberg through the DFG-Center for Functional Nanostructures (CFN) within subproject A 1.4. The project PHOME acknowledges the financial support of the Future and Emerging Technologies (FET) program within the Seventh Framework Programme for Research of the European Commission, under FET-Open grant number 213390. The project METAMAT is supported by the Bundesministerium für Bildung und Forschung (BMBF). The research of G. von Freymann is further supported through a DFG Emmy Noether fellowship (DFG-Fr 1671/4-3). The Ph.D. education of M. Thiel is embedded in the Karlsruhe School of Optics and Photonics (KSOP).

References

1. K. Robbie, M. J. Brett, and A. Lakhtakia, Nature **384**, 616 (1996).
2. A. Chutinan and S. Noda, Phys. Rev. B **57**, R2006 (1998).
3. S. R. Kennedy, M. J. Brett, O. Toader, and S. John, Nano Lett. **2**, 59 (2002).
4. K. K. Seet, V. Mizeikis, S. Matsuo, S. Juodkazis, and H. Misawa, Adv. Mater. **17**, 541 (2005).
5. Y. K. Pang, J. C. W. Lee, H. F. Lee, W. Y. Tam, C. T. Chan, and P. Sheng, Opt. Express **13**, 7615 (2005).
6. J. Lee and C. T. Chan, Opt. Express **13**, 8083 (2005).
7. M. Thiel, M. Decker, M. Deubel, M. Wegener, S. Linden, and G. von Freymann, Adv. Mater. **19**, 207 (2007).
8. A. Lakhtakia, Optik (Stuttgart) **119**, 175 (2008).
9. M. Thiel, M. S. Rill, G. von Freymann, and M. Wegener, Adv. Mater. **21**, 4680 (2009).
10. E. Plum, J. Zhou, J. Dong, V. A. Fedotov, T. Koschny, C. M. Soukoulis, and N. I. Zheludev, Phys. Rev. B **79**, 035407 (2009).
11. S. Zhang, Y.-S. Park, J. Li, X. Lu, W. Zhang, and X. Zhang, Phys. Rev. Lett. **102**, 023901 (2009).
12. T. G. Mackay and A. Lakhtakia, Microwave Opt. Technol. Lett. **50**, 1368 (2008).
13. N. Liu, H. Liu, S. Zhu, and H. Giessen, Nat. Photonics **3**, 157 (2009).
14. M. Decker, M. Ruther, C. E. Kriegler, J. Zhou, C. M. Soukoulis, S. Linden, and M. Wegener, Opt. Lett. **34**, 2501 (2009).
15. J. K. Gansel, M. Thiel, M. S. Rill, M. Decker, K. Bade, V. Saile, G. von Freymann, S. Linden, and M. Wegener, Science **325**, 1513 (2009).
16. M. Thiel, M. Hermatschweiler, G. von Freymann, and M. Wegener, Appl. Phys. Lett. **91**, 123515 (2007).
17. D. M. Whittaker and I. S. Culshaw, Phys. Rev. B **60**, 2610 (1999).
18. S. G. Tikhodeev, A. L. Yablonskii, E. A. Muljarov, N. A. Gippius, and T. Ishihara, Phys. Rev. B **66**, 045102 (2002).